J. Fluid Mech. (1987), *vol.* 176, *pp.* 443–464
Printed in Great Britain

The unsteady motion of a drop moving vertically under gravity

By R. F. CHISNELL
Department of Mathematics, University of Manchester, Manchester M13 9PL, UK

(Received 13 November 1985 and in revised form 30 August 1986)

The unsteady flow field pertaining to a drop moving vertically under gravity is obtained from the Stokes equations applicable to low-Reynolds-number flow. A proof is given that there is no variation in the normal stress over the drop surface. In consequence unsteadily moving drops remain spherical, subject only to the criterion of low Reynolds number. Numerical results are presented for a water drop moving through air. A small-time analysis of the motion provides a comparison between the motion of any drop, or bubble, with that of the presented water-drop solution.

1. Introduction

The unsteady motion of a drop moving vertically under gravity is analysed using the Stokes equations (with retention of the time derivative) for low-Reynolds-number flow. The internal and external flow for a drop of radius a, density ρ_0 and viscosity coefficient μ_0 moving steadily under gravity is well known. In steady motion the speed of the drop is given in terms of $\sigma = \mu_1/\mu_0$, the ratio of viscosity coefficients of the medium to the drop, and the density ratio $h = \rho_0/\rho_1$, as

$$V_1 = \frac{2}{3}\frac{(1+\sigma)(h-1)}{(3+2\sigma)}\frac{a^2 g}{\nu_1}, \tag{1.1}$$

with $\nu_1 = \mu_1/\rho_1$, the kinematic viscosity of the medium.

The unsteady motion of a solid sphere has been studied by Villat (1943) and Ockendon (1968). Sy, Taunton & Lightfoot (1970) determined the speed of both a solid sphere and a bubble having zero tangential stress at the interface. This work was extended by Sy & Lightfoot (1971) to include the speed of a drop, but the work is incorrectly formulated. This paper studies the motion of a drop, or a bubble, without any limitation being placed on the density or the viscosity of the drop or of the medium, other than that each parameter is a constant. The speed of the drop is determined and in addition a description of the flow inside and outside the drop is presented as a function of time. Numerical results are presented for a water drop moving through air.

The flow is assumed known at $t = 0$ and two cases are considered. First, the drop is at rest in a quiescent medium. Secondly, the drop moves steadily for $t < 0$ with a speed V_0 which is not equal to the speed V_1 in (1.1). The second case arises if the drop is acted on by forces other than gravity, possibly electrical, for $t < 0$, and these forces are removed at $t = 0$. A steadily falling drop which encounters a sudden change in the medium, such as at an inversion in the atmosphere, will to some extent be modelled by this second case. The known initial flow enables a Laplace transform solution to be obtained.

A steadily moving drop is known to have a uniform difference in normal stress at its surface (Batchelor 1967, p. 238). In consequence, steadily moving drops retain their assumed spherical shape without requiring the imposition of a dominant surface-tension force. The difference in normal surface stress is examined in unsteady flow and is again found to be uniform. Accelerating drops governed by the Stokes equations thus have no tendency to depart from a spherical shape.

Small- and large-time results are derived from the transforms and numerical results are obtained for intermediate times after the inversion integrals have been reduced to real infinite integrals. Results are presented for the speed of the drop and a flow function, from which the streamline pattern is obtained at a sequence of times. The analytic small- and large-time results enable the motion of any drop, or bubble, moving through any medium to be compared with the presented solution for a water drop in air. For small time a boundary-layer type of flow is found near the drop surface which is obtained in terms of repeated integrals of the complementary error function. For the case of a water drop moving through air two distinct timescales affect the approach to the steady-state flow. The speed of the drop and the flow function become close to their steady-state values after a time of order $\nu_1 t/a^2 = 500$, whereas the flow pattern becomes close to the steady-state pattern after a time of only $\nu_1 t/a^2 = 5$.

2. The Laplace transform solution

A spherical drop of radius a moves vertically downwards with speed $V(t)$. The Stokes equation of motion referred to axes moving with the drop is

$$\frac{\partial \boldsymbol{v}}{\partial t} = -\frac{1}{\rho}\nabla p + \nu \nabla^2 \boldsymbol{v} - g\boldsymbol{k} + \frac{\mathrm{d}V}{\mathrm{d}t}\boldsymbol{k}, \tag{2.1}$$

where $\boldsymbol{k}$ is a unit upward vector and the density and kinematic viscosity have the values ρ_1, ν_1 outside the drop and ρ_0, ν_0, inside the drop. For axisymmetric flow the incompressible continuity equation is satisfied by a stream function ψ, with

$$v_r = \frac{1}{r^2 \sin\theta}\frac{\partial \psi}{\partial \theta}, \quad v_\theta = -\frac{1}{r \sin\theta}\frac{\partial \psi}{\partial r}, \tag{2.2}$$

r being distance from the drop centre and θ the inclination to the upward vertical. The vorticity equation derived from (2.1) is

$$\frac{\partial}{\partial t}\mathrm{D}^2\psi = \nu \mathrm{D}^4 \psi, \tag{2.3}$$

with

$$\mathrm{D}^2 = \frac{\partial^2}{\partial r^2} + \frac{\sin\theta}{r^2}\frac{\partial}{\partial \theta}\frac{1}{\sin\theta}\frac{\partial}{\partial \theta}. \tag{2.4}$$

A solution of the form

$$\psi = \sin^2\theta f(r, t) \tag{2.5}$$

exists with f satisfying

$$\mathrm{L}_1 \mathrm{L}_2 f = 0, \tag{2.6}$$

where

$$\mathrm{L}_1 = \frac{\partial^2}{\partial r^2} - \frac{2}{r^2}, \quad \mathrm{L}_2 = \frac{\partial^2}{\partial r^2} - \frac{2}{r^2} - \frac{1}{\nu}\frac{\partial}{\partial t}. \tag{2.7}$$

Outside the drop ($r > a$), ν has the value ν_1 and for large r

$$f(r, t) \sim \tfrac{1}{2} r^2 V(t) \tag{2.8}$$

represents the translation $V(t)$. Inside the drop ν has the value ν_0 and the fluid velocity is finite at the centre, requiring f/r^2 to be well behaved for small r. At the surface of the drop, $r = a$, the radial velocity is zero:

$$f(a_+, t) = 0, \quad f(a_-, t) = 0. \tag{2.9}$$

Also at the drop surface the azimuthal velocity v_θ and tangential stress component $p_{r\theta}$ are continuous,

$$\left.\begin{aligned} f_r(a_+, t) &= f_r(a_-, t), \\ \mu_1\left\{f_{rr}(a_+, t) - \frac{2}{a} f_r(a_+, t)\right\} &= \mu_0\left\{f_{rr}(a_-, t) - \frac{2}{a} f_r(a_-, t)\right\}, \end{aligned}\right\} \tag{2.10}$$

the r-suffix denoting differentiation.

To complete the formulation of the problem the initial flow is prescribed. The simplest case is to release the drop from rest in a quiescent medium, $f(r, 0) = 0$. Alternatively, the drop may be considered to be moving steadily with a speed V_0, different from its terminal speed V_1, for $t < 0$, and to commence its approach to the terminal speed, given by (1.1), at $t = 0$. The initial and final flow fields are then both given by the known steady-flow solution

$$\frac{f(r,0)}{V_0 a^2} = \frac{f(r,\infty)}{V_1 a^2} = \begin{cases} \frac{1}{2}\left(\frac{r^2}{a^2} - \frac{a}{r}\right) + \frac{(3+2\sigma)}{4(1+\sigma)}\left(\frac{a}{r} - \frac{r}{a}\right), & r > a, \\ \frac{\sigma r^2 (r^2 - a^2)}{4(1+\sigma)\, a^4}, & r < a, \end{cases} \tag{2.11}$$

with $\sigma = \mu_1/\mu_0$.

The solution is obtained in terms of the Laplace transform

$$\bar{f}(r, s) = \int_0^\infty \mathrm{e}^{-st} f(r, t)\, \mathrm{d}t \tag{2.12}$$

and is expressed for $t > 0$ as the sum of two parts

$$f = f_1 + f_2, \tag{2.13}$$

where

$$\mathrm{L}_1 f_1 = 0, \quad \mathrm{L}_2 f_2 = 0. \tag{2.14a, b}$$

The initial flow field is decomposed with

$$f_1(r, 0) = \begin{cases} \frac{1}{2} V_0 a^2 \left(\frac{r^2}{a^2} - \frac{a}{r}\right), & r > a, \\ 0, & r < a, \end{cases} \tag{2.15}$$

and the remaining terms in (2.11) comprising $f_2(r, 0)$. The transform of (2.14b) is

$$\left(\frac{\partial^2}{\partial r^2} - \frac{2}{r^2} - \frac{s}{\nu}\right)\bar{f}_2(r, s) + \frac{1}{\nu} f_2(r, 0) = 0, \tag{2.16}$$

which has

$$\bar{f}_2(r, s) = \begin{cases} \frac{V_0 a^2 (3+2\sigma)}{4s(1+\sigma)}\left(\frac{a}{r} - \frac{r}{a} + \frac{2\nu_1}{sar}\right) + A\, \mathrm{e}^{-s_1(r/a-1)}\left(\frac{a}{r} + s_1\right), & r > a, \\ \frac{V_0 \sigma}{4s(1+\sigma)\, a^2}\left(r^4 - a^2 r^2 + 10\frac{\nu_0 r^2}{s}\right) + B\left(\frac{a}{r}\sinh s_0 \frac{r}{a} - s_0 \cosh s_0 \frac{r}{a}\right), & r < a, \end{cases} \tag{2.17}$$

as a solution, where

$$s_0 = a\left(\frac{s}{\nu_0}\right)^{\frac{1}{2}}, \quad s_1 = a\left(\frac{s}{\nu_1}\right)^{\frac{1}{2}}, \tag{2.18}$$

have positive real parts in the s-plane cut along the negative real axis. The first part of each expression in (2.17) is a particular integral and the second part containing A or B is a complementary function well behaved for large or small r. The equation $\mathrm{L}_1 f_1 = 0$ is unaltered by the transformation; a solution with appropriate behaviour for large and small r and which when added to $\bar{f}_2$ satisfies (2.9) is

$$\bar{f}_1 = \begin{cases} \frac{1}{2}\overline{V}(s)\left(r^2 - \frac{a^3}{r}\right) - \frac{V_0(3+2\sigma)\nu_1}{2s^2(1+\sigma)}\frac{a}{r} - A\frac{a}{r}(1+s_1), & r > a, \\ -\frac{5V_0\sigma\nu_0}{2s^2(1+\sigma)}\frac{r^2}{a^2} - B\frac{r^2}{a^2}(\sinh s_0 - s_0\cosh s_0), & r < a. \end{cases} \tag{2.19}$$

The remaining boundary conditions, (2.10), determine A and B as

$$\left.\begin{aligned} A &= \frac{3\nu_1(T_2+2\sigma T_1)(\overline{V}-V_0/s)}{2s\{T_2+\sigma(3+s_1)T_1\}}, \\ B &= \frac{3\sigma a^2(1+s_1)(\overline{V}-V_0/s)}{2\{T_2+\sigma(3+s_1)T_1\}}, \end{aligned}\right\} \tag{2.20}$$

with

$$\left.\begin{aligned} T_1 &= 3s_0\cosh s_0 - (3+s_0^2)\sinh s_0 = -\sum_{n=0}^{\infty}\frac{s_0^{5+2n}}{(5+2n)(3+2n)(2n+1)!}, \\ T_2 &= (6+3s_0^2)\sinh s_0 - (6+s_0^2)s_0\cosh s_0 = -\sum_{n=0}^{\infty}\frac{s_0^{5+2n}}{(5+2n)(2n+1)!}, \end{aligned}\right\} \tag{2.21}$$

the series expansions being given for later use. The flow transform function $\bar{f}$ has now been determined in terms of $\overline{V}$ and to complete the transform solution $\overline{V}$ is determined by the equation of motion of the drop

$$M\frac{\mathrm{d}V}{\mathrm{d}t} = Mg - F, \tag{2.22}$$

where $M = \frac{4}{3}\pi\rho_0 a^3$ is the drop mass and F is the force exerted by the exterior fluid on the drop,

$$F = \int_0^{\pi}(p_{rr}\cos\theta - p_{r\theta}\sin\theta)\,2\pi a^2\sin\theta\,\mathrm{d}\theta. \tag{2.23}$$

The stress components

$$\left.\begin{aligned} p_{rr} &= -p + 2\mu\frac{\partial v_r}{\partial r}, \\ p_{r\theta} &= \mu\left\{r\frac{\partial}{\partial r}\left(\frac{v_\theta}{r}\right) + \frac{1}{r}\frac{\partial v_r}{\partial\theta}\right\}, \end{aligned}\right\} \tag{2.24}$$

are needed at $r = a_+$. The θ-component of (2.1) is used to determine p, and the θ-dependence is removed by writing

$$p_{rr} = -p_1 + p'_{rr}\cos\theta, \quad p_{r\theta} = p'_{r\theta}\sin\theta, \tag{2.25}$$

with p_1 a constant.

There follows

$$p'_{rr} = \rho_1 f_{rt} - \frac{\mu_1}{a^3}(a^3 f_{rrr} - 6af_r + 12f) + \rho_1 a\left(g - \frac{\mathrm{d}V}{\mathrm{d}t}\right), \tag{2.26a}$$

$$p'_{r\theta} = -\frac{\mu_1}{a^3}(a^2 f_{rr} - 2af_r + 2f), \tag{2.26b}$$

$$F = \frac{M}{\rho_0 a}(p'_{rr} - 2p'_{r\theta}), \tag{2.26c}$$

all functions being evaluated at $r = a_+$. Substituting for $\bar{f}$ in terms of $\overline{V}$ in the transform of (2.22) and (2.26) yields an equation for the speed of the drop. In steady flow the result is (1.1), and in unsteady flow the result is

$$\overline{V} - \frac{V_0}{s} = \frac{g(h-1) - \dfrac{3\nu_1 V_0(3+2\sigma)}{2(1+\sigma)a^2}}{s\left[(h+\frac{1}{2})s + \dfrac{9\nu_1(1+s_1)(T_2+2\sigma T_1)}{2a^2\{T_2+\sigma(3+s_1)T_1\}}\right]}, \tag{2.27}$$

with $h = \rho_0/\rho_1$. Introducing the steady-state speed V_1, (1.1), the equation may be recast

$$\frac{\overline{V} - V_0/s}{V_1 - V_0} = \frac{3(3+2\sigma)}{2(1+\sigma)s}\left[(h+\tfrac{1}{2})s_1^2 + \frac{9}{2}\left\{\frac{1}{1+s_1} + \frac{\sigma T_1}{T_2+2\sigma T_1}\right\}^{-1}\right]^{-1}. \tag{2.28}$$

Substitution of this result into (2.17), (2.19) and (2.20) yields the transform of the flow function; the inversion of the transforms is considered in §5.

In an earlier formulation of the $\overline{V}$ transform, (Sy & Lightfoot 1971), the kinematic viscosity ν_1 was unfortunately assumed both for the exterior and interior flow in the field equation (2.3), though the boundary conditions were correctly applied. In consequence T_1 and T_2 occurring in (2.28), though still having the functional form given in (2.21), become functions of s_1 instead of s_0. In the limiting cases of a solid sphere, $\sigma = 0$, and of a bubble, $\sigma = \infty$, T_1 and T_2 disappear from the transform and the earlier formulation remains valid.

We conclude this section by formulating a drag coefficient for the drop. The force F exerted by the exterior fluid on the drop is given by (2.22) and consists of a buoyancy term $\frac{4}{3}\pi a^3 \rho_1 g$ together with a drag

$$D = \tfrac{4}{3}\pi a^3 \rho_1 \left\{g(h-1) - h\frac{\mathrm{d}V}{\mathrm{d}t}\right\}. \tag{2.29}$$

A drag coefficient C_D based on the final steady fall of the drop is

$$C_D = \frac{D}{\frac{1}{2}\rho_1 V_1^2 \pi a^2}, \tag{2.30}$$

and (1.1) enables this to be written as

$$C_D = \frac{8(3+2\sigma)}{R(1+\sigma)}\left\{1 - \frac{h}{(h-1)g}\frac{\mathrm{d}V}{\mathrm{d}t}\right\}, \tag{2.31}$$

where $R = 2aV_1/\nu_1$ is the Reynolds number. When the drop has ceased accelerating, this result recovers the known steady-flow value (Harper 1972).

3. The normal stress at the interface

A notable feature of the motion of a drop moving steadily with speed given by (1.1) is that the difference in normal stress at the interface has no angular dependence. The normal stress components can differ only by a constant and in consequence there is no tendency for the drop to depart from an assumed spherical shape. In this section it is shown that this result also holds in unsteady flow.

To investigate the possible angular dependence of the difference in normal stress we express both $p'_{rr}(a_+, t)$ and $p'_{rr}(a_-, t)$, defined in (2.25), in terms of conditions inside the drop. Equation (2.26c) is used for $p'_{rr}(a_+, t)$, making use of (2.22) and the continuity of $p'_{r\theta}$ at the interface. Replacing ρ_1, μ_1 by ρ_0, μ_0 in (2.26a, b), provides equations for $p'_{rr}(a_-, t), p'_{r\theta}(a_-, t)$, and there follows

$$p'_{rr}(a_+, t) - p'_{rr}(a_-, t) = -\rho_0 f_{rt} + \frac{\mu_0}{a^3}(a^3 f_{rrr} - 2a^2 f_{rr} - 2a f_r + 8f), \tag{3.1}$$

the right-hand side being evaluated at $r = a_-$. Introducing $\mathrm{L}_1, \mathrm{L}_2$ from (2.7) and noting that $f(a_-, t) = 0$, the equation becomes

$$p'_{rr}(a_+, t) - p'_{rr}(a_-, t) = \mu_0 \frac{\partial}{\partial r}(\mathrm{L}_2 f) - \frac{2\mu_0}{a}\mathrm{L}_1 f. \tag{3.2}$$

Expressing f as the sum of its two parts, (2.13), and then interchanging L_1 and L_2 by use of

$$\mathrm{L}_1 - \mathrm{L}_2 = \frac{1}{\nu}\frac{\partial}{\partial t}, \tag{3.3}$$

the equation becomes

$$p'_{rr}(a_+, t) - p'_{rr}(a_-, t) = -\rho_0 \frac{\partial}{\partial t}\left\{\frac{\partial f_1}{\partial r}(a_-, t) + 2 f_2(a_-, t)\right\}. \tag{3.4}$$

Finally from (2.9) $f_2(a_-, t) = -f_1(a_-, t)$ and inside the drop (2.19) gives $f_1 \propto r^2$ so that the right-hand side of (3.4) is zero. Hence, even in unsteady motion, there can be no angular variation in the difference in normal stress across the drop surface. There can exist only a constant difference normal stress and this is determined by the surface tension. It has previously been reported, (Sy & Lightfoot 1971) and (Clift, Grace & Weber 1978, p. 295), that in addition to the assumption of low Reynolds number, the Weber number must also be small in order to ensure a spherical drop in unsteady motion. The work of this section shows that provided the motion may be described by the Stokes equations the drop remains spherical; this requires only the assumption of low Reynolds number. In steady flow Taylor & Acrivos (1964) showed that the second term in a Reynolds-number expansion gives a spheroidal shape, with a coefficient proportional to the Weber number. A similar situation may well exist in unsteady flow.

4. Small- and large-time results

The flow description for small values of the time is obtained by considering the transform functions for large values of $|s|$. The behaviour of the ratio T_2/T_1 follows from the definitions (2.21) as

$$\frac{T_2}{T_1} = s_0 + \frac{3}{s_0} + O(s_0^{-2}). \tag{4.1}$$

Substitution into (2.28) and inverting the transform yields a series expansion in powers of $t^{\frac{1}{2}}$. The first three terms are

$$\frac{V(t)-V_0}{V_1-V_0}=\frac{3(3+2\sigma)\,\nu_1 t}{2(1+\sigma)\,(h+\frac{1}{2})\,a^2}\Bigg[1-\frac{6(\nu_1 t/\pi a^2)^{\frac{1}{2}}}{(h+\frac{1}{2})\{1+\sigma(\nu_0/\nu_1)^{\frac{1}{2}}\}}+\frac{9\nu_1 t\left\{\frac{9}{2}-(h+\frac{1}{2})\left(1+2\sigma^2\frac{\nu_0}{\nu_1}\right)\right\}}{4(h+\frac{1}{2})^2 a^2\{1+\sigma(\nu_0/\nu_1)^{\frac{1}{2}}\}^2}\cdots\Bigg]. \tag{4.2}$$

This three-term series is shown in figure 2 for a water drop in air and is in satisfactory agreement with the numerical solution for $\nu_1 t/a^2$ less than 100.

The small-time behaviour of the flow inside the drop similarly follows from the transforms of §2. The leading term in the large-$|s|$ analysis is proportional to $s^{-\frac{1}{4}}\{\exp(r-a)\,s_0/a-r^2/a^2\}$ and both terms in the bracket need to be kept to describe the boundary layer near $r=a$. In terms of the coordinate

$$\eta=\frac{a-r}{2(\nu_0 t)^{\frac{1}{2}}}, \tag{4.3}$$

and successive integrals of the complementary error function $i^n\operatorname{erfc}\eta$, the first three terms are

$$\frac{f(r,t)-f(r,0)}{(V_1-V_0)\,a^2}=\frac{9}{4}\frac{(3+2\sigma)}{(1+\sigma)\,h(h+\frac{1}{2})\{1+\sigma(\nu_0/\nu_1)^{\frac{1}{2}}\}}\left(\frac{\nu_1 t}{a^2}\right)^{\frac{3}{4}}\left\{f_1+\left(\frac{\nu_1 t}{a^2}\right)^{\frac{1}{4}}f_2+\frac{\nu_1 t}{a^2}f_3\cdots\right\}, \tag{4.4}$$

where

$$\left.\begin{aligned}
f_1&=8\mathrm{i}^3\operatorname{erfc}\eta-\frac{4}{3\pi^{\frac{1}{2}}}\frac{r^2}{a^2},\\
f_2&=(1+c)\left(16\mathrm{i}^4\operatorname{erfc}\eta-\frac{r^2}{2a^2}\right)-\left(\frac{\nu_0}{\nu_1}\right)^{\frac{1}{4}}\left(16\frac{a}{r}\mathrm{i}^4\operatorname{erfc}\eta-\frac{r^2}{2a^2}\right),\\
f_3&=\left(32\mathrm{i}^5\operatorname{erfc}\eta-\frac{4}{15\pi^{\frac{1}{2}}}\frac{r^2}{a^2}\right)\left\{c^2+c-d-(1+c)\frac{a}{r}\left(\frac{\nu_0}{\nu_1}\right)^{\frac{1}{4}}\right\}+\frac{4}{15\pi^{\frac{1}{2}}}(1+c)\left(\frac{\nu_0}{\nu_1}\right)^{\frac{1}{4}}\left(\frac{r^2}{a^2}-\frac{r}{a}\right),
\end{aligned}\right\} \tag{4.5}$$

and

$$c=3\left(\frac{\nu_0}{\nu_1}\right)^{\frac{1}{4}}-\frac{3\left\{\sigma\left(\frac{\nu_0}{\nu_1}\right)^{\frac{1}{4}}+\frac{3}{2h+1}\right\}}{1+\sigma(\nu_0/\nu_1)^{\frac{1}{2}}},$$

$$d=\frac{3[\{2+\sigma(\nu_0/\nu_1)^{\frac{1}{2}}-3\sigma\}\,\nu_0/\nu_1+3\{1+(2\sigma-3)\,(\nu_0/\nu_1)^{\frac{1}{4}}\}/(2h+1)]}{1+\sigma(\nu_0/\nu_1)^{\frac{1}{2}}}.$$

This three-term expansion has been used to compute f in the case of a water drop starting from rest at $t=0.05a^2/\nu_1$ and the results agree to within 1% with the numerical results presented later; the result is shown in figure 3 (*a*).

Of particular interest in the flow inside the drop is the location of the turning point of $f(r,t)$. At this value of $r=r_{\mathrm{M}}$, (2.2) shows $v_\theta=0$, and in the equatorial plane $\theta=\frac{1}{2}\pi$ it locates stagnation points as v_r also vanishes. Inside the drop the fluid circulates around a circle of radius r_{M} in the equatorial plane. In steady flow (2.11) shows that $r_{\mathrm{M}}=a/\sqrt{2}$. In unsteady flow starting with a drop at rest, $f(r,0)=0$, the location of r_{M} in the equatorial plane starts on the surface of the drop, $r_{\mathrm{M}}=a$, and moves inwards

towards its final location at $r_M = a/\sqrt{2}$. A simple description of the motion of this equatorial stagnation circle is provided by the leading term f_1 in (4.4). An r-differentiation of f_1 leads to a turning point at the root of

$$\mathrm{i}^2 \operatorname{erfc} \eta = \frac{2}{3}\left(\frac{\nu_0 t}{\pi}\right)^{\frac{1}{2}} \frac{r}{a^2}. \tag{4.6}$$

At $\nu_0 t/a^2 = 0.46 \times 10^{-2}$, which for a water drop in air corresponds to $\nu_1 t/a^2 = 0.05$, the root is $r_M = 0.882a$. The agreement with the full numerical solution is excellent up to this value of the time, and the root is displayed in figure 4 up to $\nu_1 t/a^2 = 1$.

The flow outside the drop is similarly derived for small values of the time in terms of the similarity variable

$$\zeta = \frac{r-a}{2(\nu_1 t)^{\frac{1}{2}}}. \tag{4.7}$$

There follows

$$\frac{f(r,t)-f(r,0)}{(V_1-V_0)a^2} = \frac{3(3+2\sigma)\nu_1 t}{2(1+\sigma)(h+\frac{1}{2})a^2}\left\{f_4+\left(\frac{\nu_1 t}{a^2}\right)^{\frac{1}{2}} f_5+\frac{\nu_1 t}{a^2} f_6 \cdots\right\}, \tag{4.8}$$

where

$$\left.\begin{aligned}
f_4 &= \frac{1}{2}\left(\frac{r^2}{a^2}-\frac{a}{r}\right),\\
f_5 &= \frac{12\mathrm{i}^3 \operatorname{erfc}\zeta - \frac{2}{\pi^{\frac{1}{2}}}\left\{\frac{a}{r}+\frac{3}{2}\left(\frac{r^2}{a^2}-\frac{a}{r}\right)\Big/(h+\frac{1}{2})\right\}}{1+\sigma(\nu_0/\nu_1)^{\frac{1}{2}}},\\
f_6 &= e\left(\frac{r^2}{a^2}-\frac{a}{r}\right)+\frac{32\mathrm{i}^4 \operatorname{erfc}\zeta\left\{g+\frac{3}{4}\left(\frac{a}{r}-1\right)\right\}-g\frac{a}{r}}{1+\sigma(\nu_0/\nu_1)^{\frac{1}{2}}},\\
e &= \frac{9}{8(h+\frac{1}{2})\{1+\sigma(\nu_0/\nu_1)^{\frac{1}{2}}\}^2}\left\{\frac{9}{2(h+\frac{1}{2})}-1-2\sigma^2\frac{\nu_0}{\nu_1}\right\},\\
g &= \frac{3}{4}\left[1+\left(2-\frac{3}{1+\sigma(\nu_0/\nu_1)^{\frac{1}{2}}}\right)\sigma\left(\frac{\nu_0}{\nu_1}\right)^{\frac{1}{2}}-\frac{9}{2(h+\frac{1}{2})\{1+\sigma(\nu_0/\nu_1)^{\frac{1}{2}}\}}\right].
\end{aligned}\right\} \tag{4.9}$$

This three-term expansion is also shown in figure 3(*a*) for $\nu_1 t/a^2 = 0.05$.

It is of interest that the leading term is $O(t)$ in the external flow and $O(t^{\frac{3}{2}})$ in the internal flow and further that the leading external-flow term is a potential flow past a sphere. The scaling factor in (4.8) shows that this potential flow describes a sphere moving with an acceleration

$$\frac{\mathrm{d}V}{\mathrm{d}t} = \frac{3(3+2\sigma)(V_1-V_0)\nu_1}{2(1+\sigma)(h+\frac{1}{2})a^2}. \tag{4.10}$$

This result also follows directly from irrotational flow considerations. To maintain a steady flow with speed V_0 for $t < 0$ an applied force is required to provide a balance between the buoyancy force and the viscous drag. When the applied force is removed at $t = 0$ the drop accelerates and in the irrotational flow regime experiences an acceleration reaction $\frac{2}{3}\pi\rho_1 a^3 \,\mathrm{d}V/\mathrm{d}t$, (Batchelor 1967, p. 453). The equation of motion of the drop is

$$\tfrac{4}{3}\pi a^3\rho_0\frac{\mathrm{d}V}{\mathrm{d}t} = \tfrac{4}{3}\pi a^3(\rho_0-\rho_1)g - 2\pi a\mu_1 V_0\frac{(3+2\sigma)}{(1+\sigma)} - \tfrac{2}{3}\pi a^3\rho_1\frac{\mathrm{d}V}{\mathrm{d}t}, \tag{4.11}$$

and equation (1.1) enables this to be recast in the form (4.10).

The large-time behaviour is governed by the behaviour near the singular points of the transforms. In the next section it is shown there are no singular points in the s-plane cut along the negative real axis, so that the large-time results are governed by the behaviour of the transforms near $s = 0$. The series expansions in (2.21) show

$$\frac{T_2}{T_1} \sim 3 + \frac{s_0^2}{7} - \frac{s_0^4}{441} \dots . \tag{4.12}$$

On substitution into (2.28), the term of $O(s^{-1})$ gives the required asymptotic value V_1 for $V(t)$ and terms of $O(s^{-\frac{1}{2}}, s^{\frac{1}{2}}, s^{\frac{3}{2}})$ give the asymptotic result

$$\frac{V_1 - V(t)}{V_1 - V_0} \sim \frac{(3+2\sigma)\,a}{3(1+\sigma)\,(\pi\nu_1 t)^{\frac{1}{2}}}\left[1 + \frac{a^2}{2\nu_1 t}\left\{\frac{4(1+\sigma)}{3(3+2\sigma)}(h+\tfrac{1}{2}) - 1\right\}\right.$$
$$\left. + \frac{3a^4}{4\nu_1^2 t^2}\left\{1 + \frac{4(1+\sigma)^2\,(h+\frac{1}{2})^2}{3(3+2\sigma)^2} - \tfrac{4}{3}(h+\tfrac{1}{2})\left(\frac{6+5\sigma}{3+2\sigma} - \frac{\sigma\nu_1}{7\nu_0(3+2\sigma)^2}\right)\right\} \dots\right]. \tag{4.13}$$

The leading term is $O(\nu_1 t/a^2)^{-\frac{1}{2}}$ with a coefficient depending only on σ. However subsequent terms also depend on $a^2(1+\sigma)\,(h+\frac{1}{2})/(3+2\sigma)\,\nu_1 t$ and for a water drop moving through air the series provides a good asymptotic estimate only for extremely large values of t as h is large. In §6 numerical results are presented for a water drop in air up to $\nu_1 t/a^2 = 1500$, but as h is about 800, eleven terms in the above series would be required to provide the asymptotic estimate at this value of t. At $\nu_1 t/a^2 = 10^5$, however, the three given terms do provide agreement with all eight figures in the numerical solution for $V(t)$.

The large-time flow-field asymptotic estimate is similarly obtained. The departure from the final steady flow is $O(t^{-\frac{3}{2}})$, but because of the large value of h for a water drop in air the three-term asymptotic series does not provide a good comparison with the numerical solution over the range of time presented. In other physical situations, such as the ascent of a bubble, the large-time asymptotic series may have greater utility and the first term

$$\frac{f(r,t) - f(r,\infty)}{(V_1 - V_0)\,a^2} = \begin{cases} \dfrac{\sigma(h+\frac{1}{2})}{36(1+\sigma)}\dfrac{r^2}{a^2}\left(1 - \dfrac{r^2}{a^2}\right)\dfrac{a^3}{\pi^{\frac{1}{2}}(\nu_1 t)^{\frac{3}{2}}}, & r < a \\ -\dfrac{a^3}{\pi^{\frac{1}{2}}(\nu_1 t)^{\frac{3}{2}}}\left[\dfrac{1}{120}\left(\dfrac{r}{a} - 1\right)^3\left(\dfrac{r}{a} + 3 + \dfrac{a}{r}\right)\dfrac{(3+2\sigma)}{(1+\sigma)}\right. & \\ \qquad \left. + \tfrac{1}{36}(h+\tfrac{1}{2})\left(\dfrac{r}{a} - 1\right)\left(2\dfrac{r}{a} - \dfrac{1 + a/r}{1+\sigma}\right)\right], & r > a \end{cases} \tag{4.14}$$

is given for reference.

5. Inversion of the transforms

In §2 the Laplace transform of the speed of the drop $V(t)$ and the flow function $f(r,t)$ were obtained in the s-plane cut along the negative real axis. To obtain numerical results from the Laplace inversion theorem, the Bromwich path of integration is deformed to an infinite loop integral around the negative real axis. Before deforming the path an analysis of the singular points of $\bar{f}(r,s)$ and $\overline{V}(s)$ is required.

Singular points of $\overline{V}(s)$ will occur at zeros of the term in the square bracket in (2.28) and such points also define the singular points of $\bar{f}(r,s)$. We use the Principle of the

Argument to demonstrate that the transform functions have no poles in the cut s-plane and hence the two paths of integration are equivalent. On the cut all terms on the right-hand side of (2.28) are real with the exception of the $(1+s_1)^{-1}$ term, s_1 being purely imaginary. To facilitate an examination of the transform along the cut, the transform is rearranged to make this term more accessible,

$$\overline{V}-\frac{V_0}{s}=\frac{\frac{3}{2}\frac{(3+2\sigma)}{(1+\sigma)}(V_1-V_0)\left\{1+\frac{\sigma T_1(1+s_1)}{T_2+2\sigma T_1}\right\}}{s\left\{\frac{9}{2}+\frac{\sigma T_1 s_1^2(h+\frac{1}{2})}{T_2+2\sigma T_1}\right\}H(s)}, \tag{5.1}$$

where

$$H(s)=1+s_1+\left\{\frac{\sigma T_1}{T_2+2\sigma T_1}+\frac{9}{2s_1^2(h+\frac{1}{2})}\right\}^{-1}. \tag{5.2}$$

Apart from the origin, singularities of $\overline{V}$ are given by the zeros of $H(s)$; singularities of the $\{\ \}$ bracket in the numerator and zeros of the bracket in the denominator in (5.1) are not singularities of $\overline{V}$.

Some information about the zeros of $H(s)$ may be obtained by considering the change in the argument of $H(s)$ around the contour shown in figure 1, comprising a large and small circle centred on the origin joined by lines on either side of the negative real axis. On the small circle $H(s)$ remains close to 1. On the large circle (4.1) gives $H(s)\sim s_1+s_0/\sigma$, showing that $\operatorname{Re}H(s)>0$ on this circle. On the lines joining the circles, $\operatorname{Im}H(s)=\operatorname{Im}s_1$ which is positive on the upper line and negative on the lower line. We have thus shown that $H(s)$ is not real and negative anywhere on the contour. Consequently as s describes the contour in figure 1, $H(s)$ describes a contour that does not cross the negative real axis, and thus the change in argument of $H(s)$ is zero. The Principle of the Argument shows that the number of zeros of $H(s)$ equals the number of its poles.

The poles of $H(s)$ are located at the zeros of the function

$$I(s)=\frac{\sigma T_1}{T_2+2\sigma T_1}+\frac{9}{2s_1^2(h+\frac{1}{2})}. \tag{5.3}$$

The change in the argument of $I(s)$ around the same contour is now considered. On the small circle the second term is dominant. As the coefficient of s_1^{-2} is essentially positive, when s describes a small circle cut by the negative s-axis $I(s)$ will describe a large circle cut by the same axis. On the large circle the first term in $I(s)$ dominates, $I(s)\sim\sigma s_0^{-1}$, and $I(s)$ describes a small semicircle having a positive real part as σ is positive. On the negative real axis $I(s)$ is real and the imaginary part of $I(s)$ on the lines just on either side of the axis requires investigation. In the Appendix it is shown that T_2/T_1 has a positive imginary part when the real and imaginary parts of s_0 are both positive. In consequence the first term in $I(s)$ has a negative imaginary part on the upper line and the second term clearly has the same property. Thus on the upper line, and similarly for the lower line, $I(s)$ is nowhere real. Hence nowhere on the contour is $I(s)$ real and negative and the change in argument of $I(s)$ is zero, indicating that it has an equal number of zeros and poles. Apart from the origin, poles of $I(s)$ occur only when $T_2/T_1=-2\sigma$. However in the Appendix it is shown that T_2/T_1 can be real and negative only on the negative real s-axis. Hence $I(s)$ has no poles inside the contour of figure 1 and thus $I(s)$ has no zeros, giving $H(s)$ no zeros and hence the transform functions have no poles in the cut plane.

The path of integration in the Laplace inversion of the transform functions may now be deformed to a loop integral around the negative real axis. In the transforms

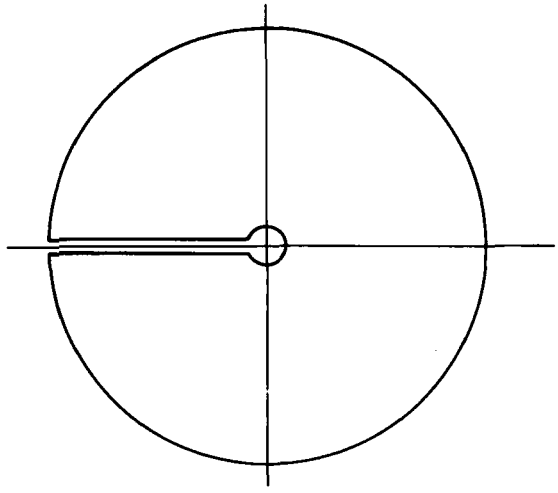

FIGURE 1. The path of integration used to consider the change in argument of the functions $H(s)$, $I(s)$ in the cut s-plane. The path consists of a small and a large circle centred on the origin and parallel lines on either side of the cut.

of both $\overline{V}$ and $\bar{f}$ the contribution from the pole at the origin produces the difference between values of the function at infinite and zero time. The integrals from the paths on each side of the axis are combined to form a single infinite integral. Writing $s = -\nu_1 x^2/a^2$, with s_0, s_1 being positive imaginary on the upper path, there follows

$$\left.\begin{aligned} \frac{V_1 - V(t)}{V_1 - V_0} &= \frac{2}{3}\frac{(3+2\sigma)}{(1+\sigma)\pi}\int_0^\infty \frac{\exp(-\nu_1 x^2 t/a^2)}{D_1^2 + x^2 D_2^2}\,\mathrm{d}x, \\ \frac{f(r,t) - f(r,\infty)}{(V_1 - V_0)a^2} &= \begin{cases} -\dfrac{2}{9}\dfrac{\sigma(3+2\sigma)(h+\frac{1}{2})}{(1+\sigma)\pi}\displaystyle\int_0^\infty \frac{N_1 x^2 \exp(-\nu_1 x^2 t/a^2)}{D_1^2 + x^2 D_2^2}\,\mathrm{d}x, & r < a, \\ \dfrac{1}{2}\left(\dfrac{r^2}{a^2} - \dfrac{a}{r}\right)\dfrac{V(t) - V_1}{V_1 - V_0} - \dfrac{(3+2\sigma)}{(1+\sigma)\pi}\displaystyle\int_0^\infty \frac{N_2 \exp(-\nu_1 x^2 t/a^2)}{x^3(D_1^2 + x^2 D_2^2)}\,\mathrm{d}x, & r > a, \end{cases} \end{aligned}\right\} \tag{5.4}$$

where

$$\left.\begin{aligned} D_1 &= 1 - \tfrac{2}{9}x^2(h+\tfrac{1}{2})\frac{T_2 + 3\sigma T_1}{T_2 + 2\sigma T_1}, \\ D_2 &= 1 - \tfrac{2}{9}x^2(h+\tfrac{1}{2})\frac{\sigma T_1}{T_2 + 2\sigma T_1}, \\ \frac{T_2}{T_1} &= \frac{(6-3y^2)\sin y - y(6-y^2)\cos y}{3y\cos y - (3-y^2)\sin y}, \\ y &= x(\nu_1/\nu_0)^{\frac{1}{2}}, \\ N_1 &= \frac{\dfrac{a}{r}\sin\dfrac{r}{a}y - y\cos\dfrac{r}{a}y - \dfrac{r^2}{a^2}(\sin y - y\cos y)}{(6-3y^2)\sin y - y(6-y^2)\cos y + 2\sigma\{3y\cos y - (3-y^2)\sin y\}}, \\ N_2 &= \left\{x\cos\left(\frac{r}{a}-1\right)x - \frac{xa}{r} - \frac{a}{r}\sin\left(\frac{r}{a}-1\right)x\right\}D_1 \\ &\quad - x\left\{\frac{a}{r}\cos\left(\frac{r}{a}-1\right)x - \frac{a}{r} + x\sin\left(\frac{r}{a}-1\right)x\right\}D_2. \end{aligned}\right\} \tag{5.5}$$

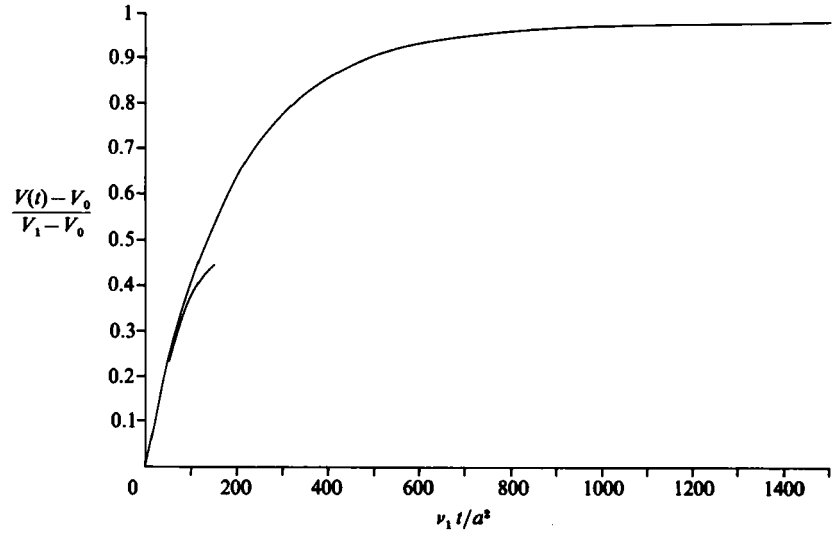

FIGURE 2. The speed of the drop $V(t)$ obtained from (5.4) is shown as a function of the non-dimensional time variable $\nu_1 t/a^2$. The initial speed of the drop is V_0 and it approaches V_1 for large time. Also shown is the three-term small-time result (4.2).

6. Results

Numerical results have been obtained for the speed of the drop and for the flow function $f(r, t)$ from the real integral formulation (5.4). Results are presented for a water drop moving through air, taking the density ratio $\rho_1/\rho_0 = h^{-1} = 1.247 \times 10^{-3}$ and the viscosity ratio $\mu_1/\mu_0 = \sigma = 176/13040$. The growth of the speed of the drop from its initial value V_0 towards its final value V_1 as a function of $\nu_1 t/a^2$ is shown in figure 2. The description given by the three-term small-time expansion (4.2) is also shown on the graph. The first term provides a timescale $2(1+\sigma)(h+\frac{1}{2})a^2/3(3+2\sigma)\nu_1$ for the development of the speed of the drop, which for the case of water drop moving through air has the value $179a^2/\nu_1$. Figure 2 shows that 0.9 of the development is completed after approximately three of these time units, or at $\nu_1 t/a^2 = 500$. For large t the departure from V_1 is $O(t^{-\frac{1}{2}})$ and is given by (4.13).

The flow function $f(r, t)$ given by (5.4) has been calculated for a sequence of t-values. Figure 3 (a, b, c) shows the growth of $f(r, t)$ in the case of a water drop starting from rest, $f(r, 0) = 0$, over a range equal to twice the drop radius. Typically the minimum value of $f(r, t)$ inside the drop is 10^{-3} times the value at $r = 2a$ and different scales of $f(r, t)$ for $r < a$ and $r > a$ have been used; the derivative of $f(r, t)$ at the interface $r = a$ is continuous. In figure 3(a) for the smallest time result presented, $\nu_1 t/a^2 = 0.05$, $f(r, t)$ has been obtained both by integration and the three-term small-time results (4.4), (4.8); the results are indistinguishable on the graph. In figure 3(c) it is seen that at $\nu_1 t/a^2 = 500$ the growth of $f(r, t)$ is almost complete and $f(r, t)$ is close to the steady-state form (2.11).

Inside the drop the fluid circulates about a circle in the equatorial plane and the radius of this circle r_M is given by the location of the minimum of $f(r, t)$. In the early stages of the flow development the minimum is close to the drop surface and in the final steady flow (2.11) shows it to be located at $r_M = a/\sqrt{2}$. The variation of r_M with t is shown in figure 4 and the estimate of r_M from a single-term small-time expansion, (4.6), is also shown.

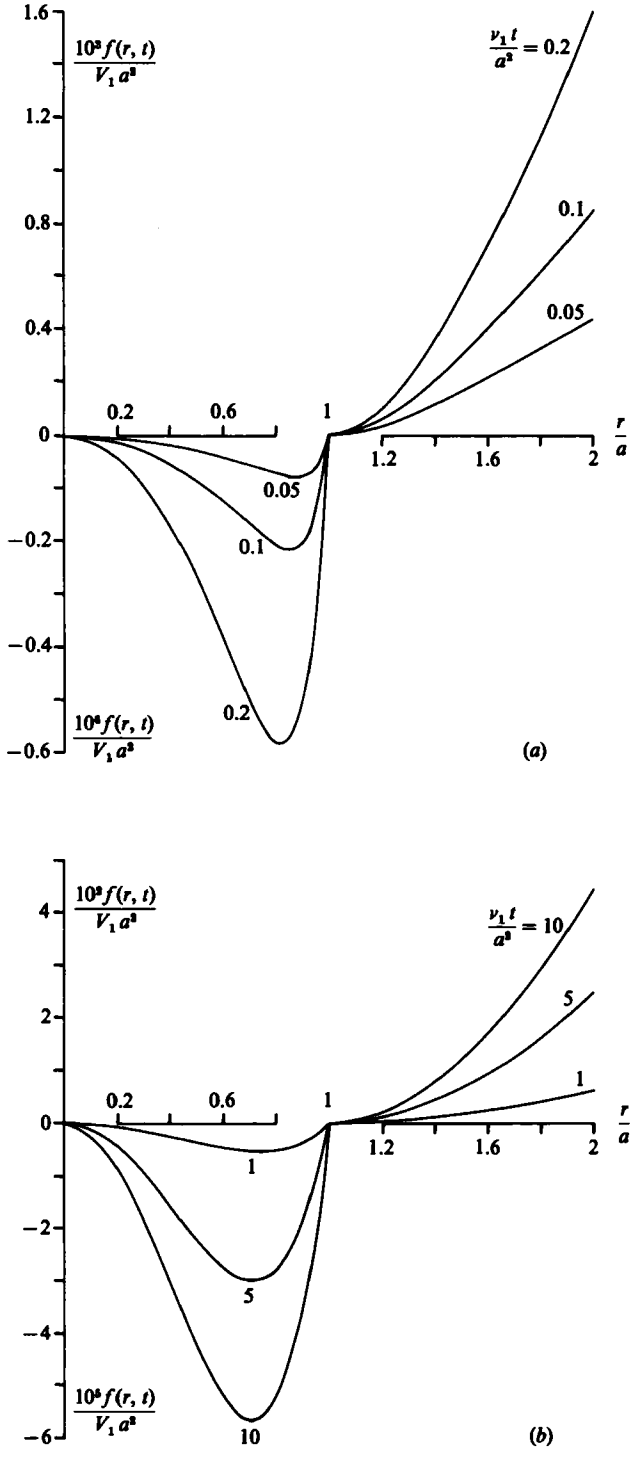

FIGURE 3(*a*,*b*) For caption see next page.

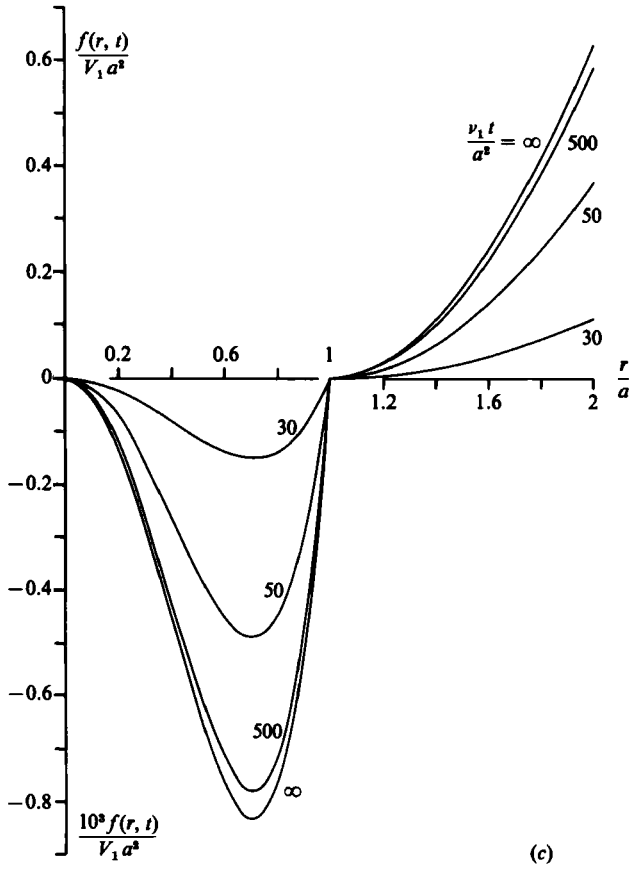

FIGURE 3(*a–c*). The flow function $f(r,t)$ given by (5.4) is shown for a sequence of values of $\nu_1 t/a^2$ over the range $r = 0, 2a$. The drop moves from rest, $f(r,0) = 0$. Scales differing by a factor of 2×10^3 or 10^3 for f have been used inside the drop $r < a$ and outside the drop $r > a$ in order to accommodate the much larger values of f in the external flow. With a uniform scale for f the slope at the surface of the drop, $r = a$, would be continuous.

It should be noted that the minimum of f approaches its final location on a much shorter timescale than that for the growth of $f(r,t)$; at $\nu_1 t/a^2 = 5$ the minimum has almost reached its final location, whereas the growth of $f(r,t)$ is only approaching completion at $\nu_1 t/a^2 = 500$. Figure 5 shows the growth of the minimum value of f over this larger timescale.

The streamlines have been drawn for a sequence of times. Apart from axial symmetry, the form (2.5) also gives symmetry about the equatorial plane, and the streamlines are shown in just one quadrant. At small values of the time the leading term of $O(t)$ is present only in the external flow. This leading term, which is the potential motion of a sphere, is shown in figure 6 with the value of ψ doubled on successive streamlines going away from the drop, starting with the streamline that crosses the equatorial plane at $r = 1.000461a$. Figures 7 (*a*, *b*, *c*) respectively show the streamline pictures at $\nu_1 t/a^2 = 0.05$, 0.2 and 5. Inside the sphere five streamlines are drawn, with ψ-values ranging from zero on the drop surface through six equal increments to the location of the minimum of $f(r,t)$ denoted by a cross. Outside the sphere the value of ψ doubles on successive lines, the streamline closest to the sphere

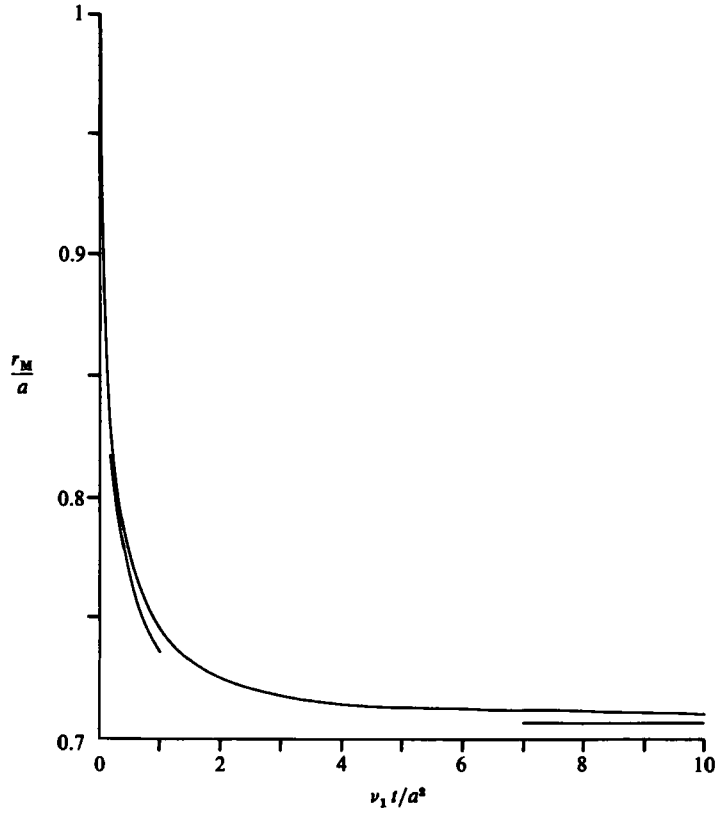

FIGURE 4. The location of the minimum r_M of the flow function f in the internal flow as a function of time. The fluid inside the drop circulates around an equatorial circle of this radius. For a drop released from rest the minimum starts on the surface and its steady state location is $r = a/\sqrt{2}$. The minimum is close to its final position by $\nu_1 t/a^2 = 5$. Also shown is the approximation obtained from the one-term small-time result (4.6).

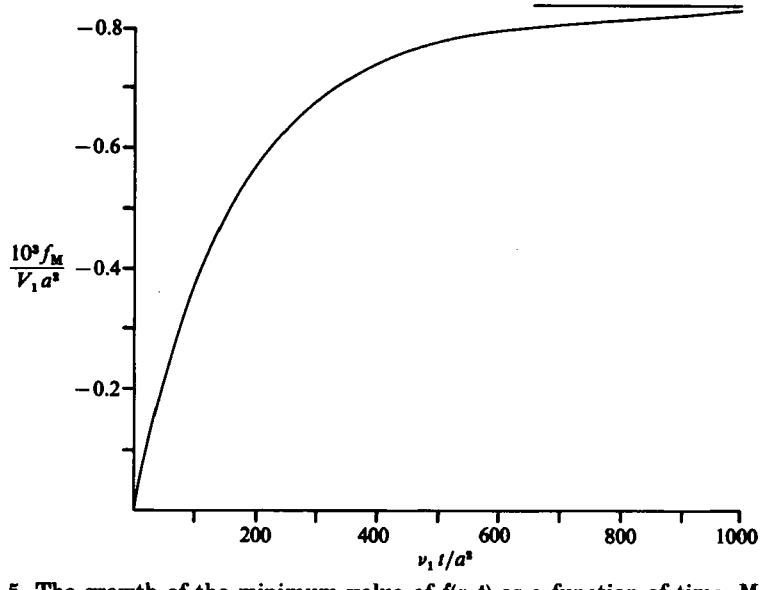

FIGURE 5. The growth of the minimum value of $f(r, t)$ as a function of time. Most of the growth takes place over a timescale $\nu_1 t/a^2 = 500$. The large-time value is $-0.832 \times 10^{-3}\ V_1\ a^2$.

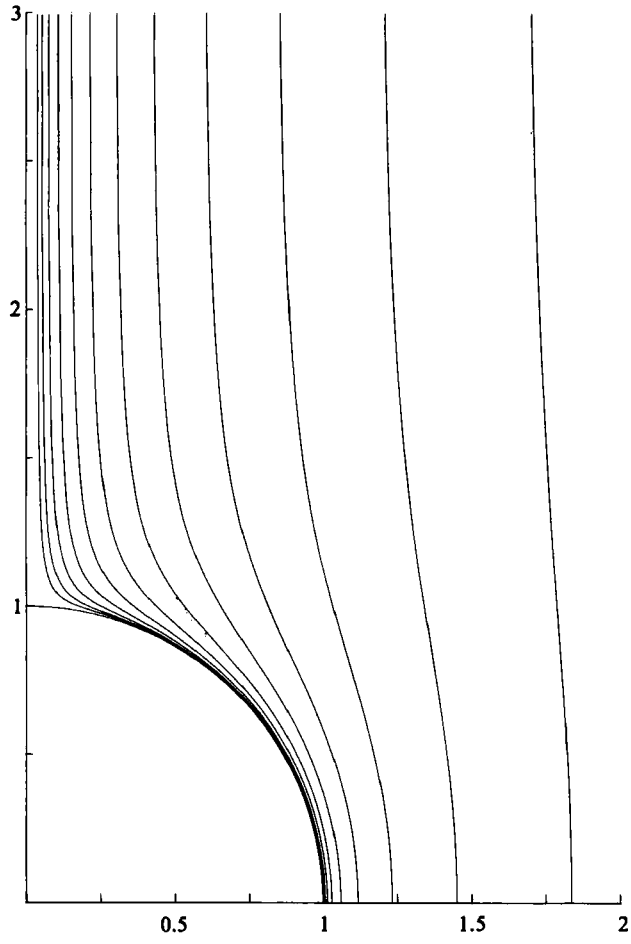

FIGURE 6. Streamlines for the potential motion of a sphere. Only one quadrant of the symmetrical flow is shown. This flow is the leading term in the small-time result (4.8). The streamline closest to the sphere meets the equatorial plane at $r = 1.000461a$ and successive streamlines double the stream-function values.

having the same magnitude of ψ as occurs at the minimum location inside the drop. As suggested by the short timescale on which the location of the minimum of f approaches its steady-state location, the streamlines are observed to approach their final pattern quickly. The streamlines at $\nu_1 t/a^2 = 5$ are close to the steady-state pattern, which is shown for comparison in figure 8.

Some insight into these two different timescales is obtained by a comparison of the initial growth of appropriate functions. It is found that there are three distinct timescales for the development of the flow, though in the case of a water drop moving through air from rest there are just two times at which various flow variables essentially complete their development. Equation (4.8) shows that the exterior-flow function is governed by the same timescale as has already been obtained for $V(t)$ and figure 3(*c*) shows that 0.9 of the development of the exterior-flow function is also completed at approximately $\nu_1 t/a^2 = 500$. The internal flow, which has a more complicated initial behaviour, may be characterized by the location of the minimum of the flow function and this minimum value. The leading term in the small-time

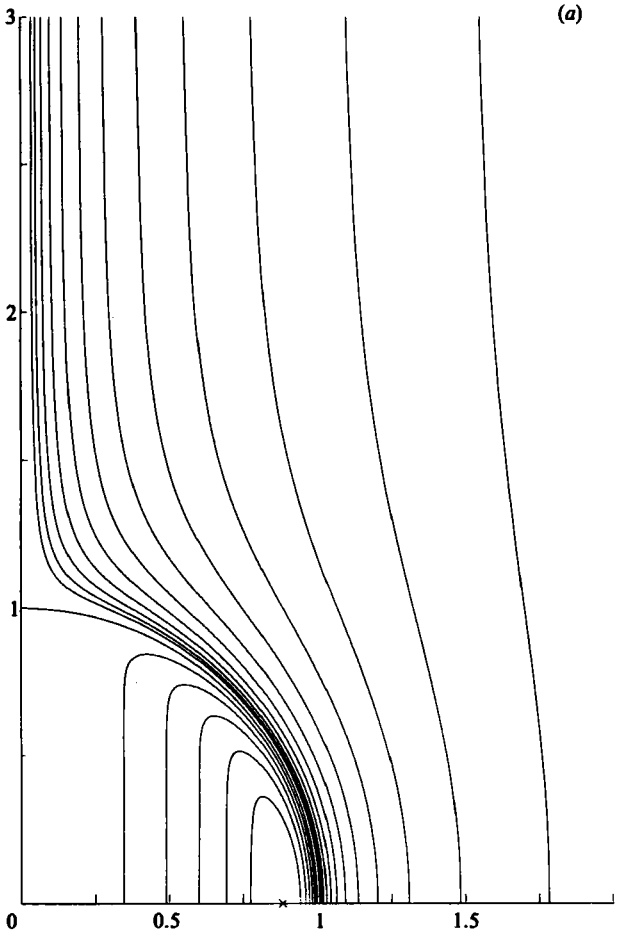

FIGURE 7. Streamline patterns at (*a*) $\nu_1 t/a^2 = 0.05$, (*b*) 0.2 and (*c*) 5 derived from (2.5) and (5.4) (see overleaf for *b*, *c*). Inside the sphere the location of the minimum value f_M of the stream function is marked ×, and five streamlines, separated by increments of $\frac{1}{6}f_M$ are shown, ψ being zero on the sphere. In the external flow the streamline closest to the sphere has a stream-function value equal and opposite to the internal minimum and successive streamlines double the stream-function value.

expansion (4.4) of the interior flow has a minimum located at the root of (4.6). This equation defines the location of the minimum r_M/a solely in terms of $\nu_0 t/a^2$. The appropriate timescale is thus a^2/ν_0 and the other physical parameters affect only the higher-order description of the motion. This timescale cannot be related to the initial speed of the minimum due to a singularity; for small t, (4.6) provides

$$r_M \sim a - 2(\nu_0 t)^{\frac{1}{2}} \ln^{\frac{1}{2}} \frac{3a}{8(\nu_0 t)^{\frac{1}{2}}}. \tag{6.1}$$

The location of the minimum, as given by (4.6), does not attain the final value of $a/\sqrt{2}$, though 0.9 of the change in r_M is achieved by $\nu_0 t/a^2 = 0.09$. For a water drop in air this time corresponds to $\nu_1 t/a^2 = 0.98$ and figure 4 shows that this fraction of the displacement of r_M is in fact completed after about five of these time units. Finally, the development of the minimum of the internal-flow function is obtained by substituting $r = r_M$ into (4.4). The steady-state minimum occurs at $a/\sqrt{2}$ and the

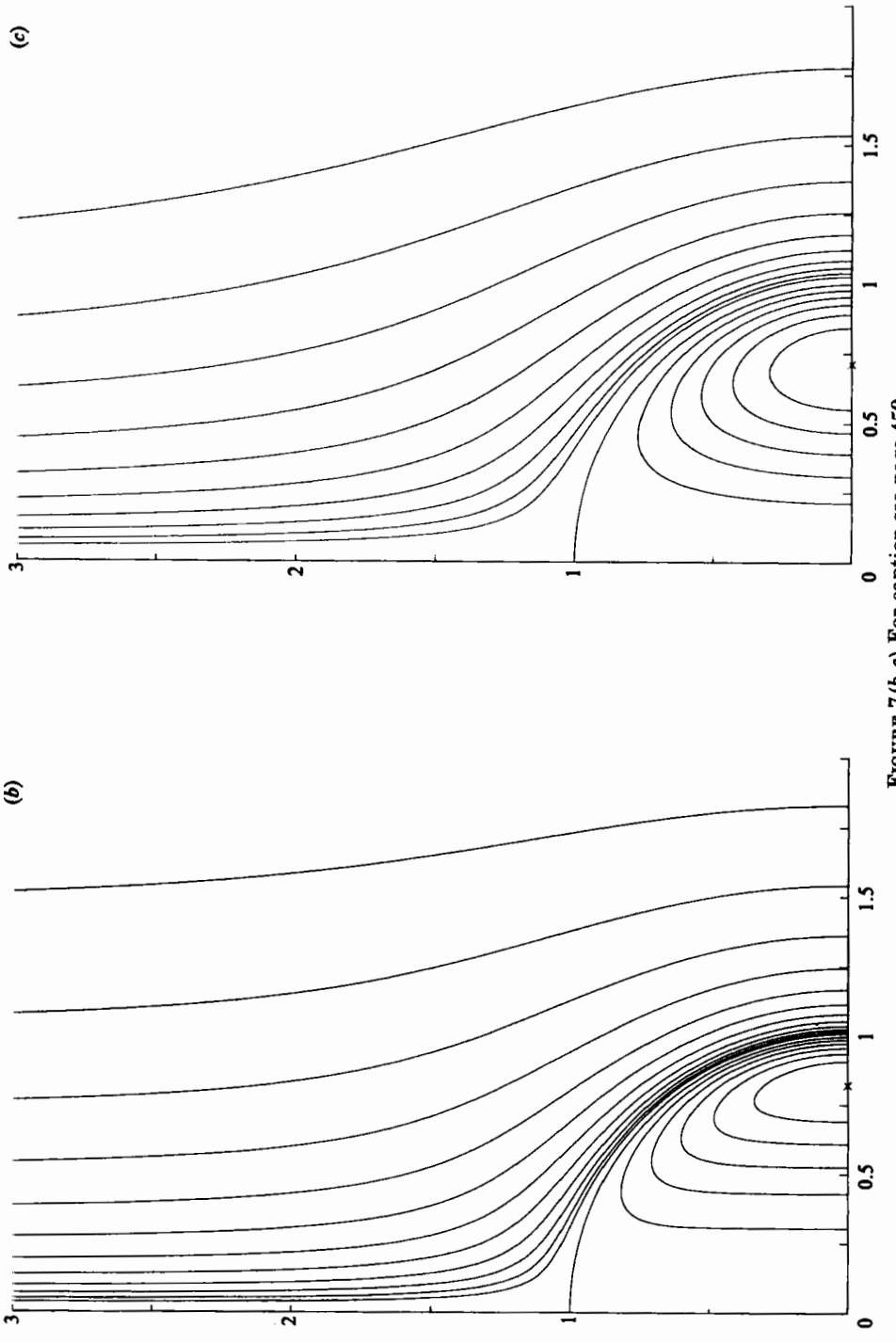

FIGURE 7 (*b*,*c*) For caption see page 459.

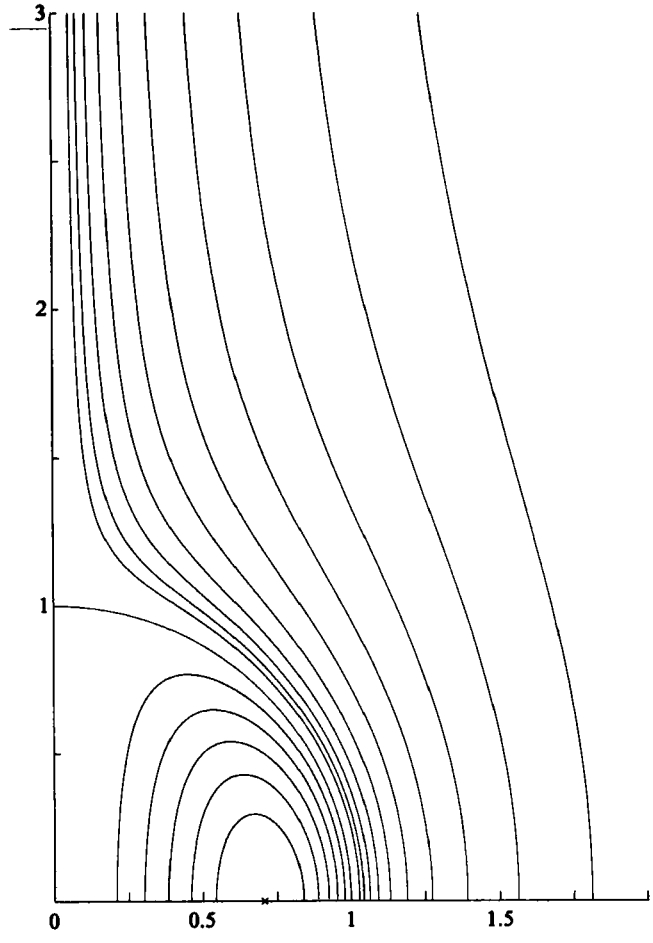

FIGURE 8. The large-time streamline pattern obtained from (2.5) and (2.11).

minimum value is obtained from (2.11) as $-V_1 a^2\sigma/16(1+\sigma)$. For a drop moving from rest, normalization of (4.4) with respect to this value gives

$$\frac{f(r_M, t)}{f(a/\sqrt{2}, \infty)} = -\frac{36(3+2\sigma)}{\sigma h(h+\frac{1}{2})\{1+\sigma(\nu_0/\nu_1)^{\frac{1}{2}}\}} \left(\frac{\nu_1 t}{a^2}\right)^{\frac{3}{2}} \{f_1(r_M, t)+\ldots\}, \tag{6.2}$$

and this coefficient provides a distinct third timescale of the motion. The $t^{\frac{3}{2}}$ behaviour is not noticeable on the timescale used in figure 5 and an estimate of the development of the internal-flow function based solely on the first term in the expansion (6.2) must be used with caution. In the case of a water drop moving through air, this single term estimates that the development is completed at $\nu_1 t/a^2 = 37.2$. Figures 3(*c*) and 5 show that 0.9 of the development takes about 13 of these units, i.e. at $\nu_1 t/a^2 = 500$. Thus although the initial timescales for the growth of the internal- and external-flow functions are different, the flow developments are essentially completed at approximately the same time. For other choices of the parameters σ and h this is unlikely to be the case and the ordering of the three timescales may well be completely different.

The author is indebted to Dr T. L. Freeman for a numerical study of the integrals in (5.4) and to Martyn Emerson for obtaining the results presented in §6 using the Nag library integration routine D01AJF and the Nag graphics library routine J06GFF.

Appendix

The inversion of the transforms presented in §5 required two properties of the functions $T_1(s_0), T_2(s_0)$, defined in (2.21). These properties, which relate to the imaginary part of T_2/T_1, are now derived.

Write $s_0 = x + \mathrm{i}y$ and determine the real and imaginary parts of T_1 and T_2:

$$\left.\begin{aligned}
\operatorname{Re} T_1 &= 3x\cosh x\cos y - 3y\sinh x\sin y \\
&\quad -(3+x^2-y^2)\sinh x\cos y + 2xy\cosh x\sin y, \\
\operatorname{Im} T_1 &= 3x\sinh x\sin y + 3y\cosh x\cos y \\
&\quad -(3+x^2-y^2)\cosh x\sin y - 2xy\sinh x\cos y, \\
\operatorname{Re} T_2 &= (6+3x^2-3y^2)\sinh x\cos y - 6xy\cosh x\sin y \\
&\quad -x(6+x^2-3y^2)\cosh x\cos y + y(6+3x^2-y^2)\sinh x\sin y, \\
\operatorname{Im} T_2 &= 6xy\sinh x\cos y + (6+3x^2-3y^2)\cosh x\sin y \\
&\quad -x(6+x^2-3y^2)\sinh x\sin y - y(6+3x^2-y^2)\cosh x\cos y.
\end{aligned}\right\} \tag{A 1}$$

The imginary part of T_2/T_1 may now be obtained and we show that for $x > 0, y > 0$, the imaginary part of T_2/T_1 is positive. This is achieved by a decomposition of the imaginary part into six positive functions. Apart from the positive factor $(T_1\overline{T}_1)^{-1}$, the imaginary part of T_2/T_1 may be written as

$$xy[y^2t_1(x) + x^2t_2(y) + y^4t_3(x) + x^4t_4(y) + t_5(x) + t_6(y)], \tag{A 2}$$

where

$$\left.\begin{aligned}
t_1(x) &= x\sinh 2x - 3\cosh 2x && +\{3+4x^2+\tfrac{2}{3}x^4\}, \\
t_2(y) &= -y\sin 2y - 3\cos 2y && +\{3-4y^2+\tfrac{2}{3}y^4\}, \\
t_3(x) &= \frac{\sinh 2x}{2x} && -\left\{1+\tfrac{2}{3}x^2+\frac{2^4}{5!}x^4\right\}, \\
t_4(y) &= -\frac{\sin 2y}{2y} && +\left\{1-\tfrac{2}{3}y^2+\frac{2^4}{5!}y^4\right\}, \\
t_5(x) &= (6x+\tfrac{1}{2}x^3)\sinh 2x - 3(1+x^2)\cosh 2x && +\{3-3x^2-x^4\}, \\
t_6(y) &= (6y-\tfrac{1}{2}y^3)\sin 2y + 3(1-y^2)\cos 2y && -\{3+3y^2-y^4\}.
\end{aligned}\right\} \tag{A 3}$$

The terms in brackets do not arise in the derivation of the imaginary part of T_2/T_1; they are introduced to render each t-function positive for positive argument and they have a zero sum after the scaling in (A 2).

The three x-functions are each seen to be positive for positive x by inspection of their power series;

$$\left.\begin{aligned} t_1(x) &= \sum_{p=4}^{\infty} \frac{2^{2p}(p-3)}{(2p)!} x^{2p}, \\ t_3(x) &= \sum_{p=3}^{\infty} \frac{2^{2p}}{(2p+1)!} x^{2p}, \\ t_5(x) &= \sum_{p=5}^{\infty} \frac{(p-3)(p-4)\,2^{2p-3}}{p(2p-2)!} x^{2p}. \end{aligned}\right\} \tag{A 4}$$

The demonstration that each y-function is positive for positive y is more tedious. The function $t_2(y)$ has

$$\frac{\mathrm{d}^6 t_2(y)}{\mathrm{d}y^6} = 64y \sin 2y \tag{A 5}$$

and the first non-zero derivative at $y = 0$ is

$$\frac{\mathrm{d}^8 t_2(0)}{\mathrm{d}y^8} = 2^8. \tag{A 6}$$

This sixth derivative is positive in $(0, \frac{1}{2}\pi)$ and as the first five derivatives are zero at the origin, an application of Taylor's theorem with a sixth-term remainder shows that $t_2(y)$ is positive in the range $(0, \frac{1}{2}\pi)$. A similar application to the first five derivatives of $t_2(y)$ shows that all these derivatives are also positive at $y = \frac{1}{2}\pi$. A similar argument may now be applied to the fourth derivative

$$\frac{\mathrm{d}^4 t_2(y)}{\mathrm{d}y^4} = -16y \sin 2y - 16 \cos 2y + 16 \tag{A 7}$$

in the range $(\frac{1}{2}\pi, \frac{3}{4}\pi)$. This derivative is positive in the range and the function and lower derivatives are positive at $\frac{1}{2}\pi$. Taylor's theorem gives that $t_2(y)$ and its first four derivatives are positive up to $y = 3\pi/4$. Similar considerations applied to the third derivative

$$\frac{\mathrm{d}^3 t_2(y)}{\mathrm{d}y^3} = -12 \sin 2y + 8y \cos 2y + 16y \tag{A 8}$$

in the range $(\frac{3}{4}\pi, \pi)$ gives $t_2(\pi) > 0$. Finally, for all $y > 0$

$$t_2(y) > -y - 3 + \{3 - 4y^2 + \tfrac{2}{3}y^4\} \tag{A 9}$$

which is positive for $y > \pi$. Hence $t_2(y)$ is positive for $y > 0$.

The function $yt_4(y)$ has its first four derivatives zero at $y = 0$ and

$$\frac{\mathrm{d}^5\{yt_4(y)\}}{\mathrm{d}y^5} = 2^4(1 - \cos 2y), \tag{A 10}$$

which is positive for all y. Hence $yt_4(y)$; and thus $t_4(y)$, is positive for $y > 0$.

To show $t_6(y)$ is positive the following derivatives are required:

$$\left.\begin{aligned}
\frac{\mathrm{d}^3 t_6(y)}{\mathrm{d}y^3} &= -(6y^2+15)\sin 2y+(4y^3+6y)\cos 2y+24y,\\
\frac{\mathrm{d}^4 t_6(y)}{\mathrm{d}y^4} &= -(8y^3+24y)\sin 2y-24\cos 2y+24,\\
\frac{\mathrm{d}^6 t_6(y)}{\mathrm{d}y^6} &= 16(2y^3+3y)\sin 2y-96y^2\cos 2y,\\
\frac{\mathrm{d}^8 t_6(y)}{\mathrm{d}y^8} &= 128\{(6y-y^3)\sin 2y+6y^2\cos 2y\}.
\end{aligned}\right\} \qquad \text{(A 11)}$$

The first non-zero derivative of $t_6(y)$ at $y = 0$ is the tenth derivative, which is positive at $y = 0$. Applications of Taylor's theorem in the same manner as for $t_2(y)$ achieve the following results. In the range $(0, \frac{1}{4}\pi)\, t_6(y)$ and its first eight derivatives are positive, in $(\frac{1}{4}\pi, \frac{1}{2}\pi)\, t_6$ and the first six derivatives are positive, in $(\frac{1}{2}\pi, \frac{3}{4}\pi)\, t_6$ and the first four derivatives are positive, in $(\frac{3}{4}\pi, \pi)\, t_6$ is positive. In the range $(\pi, \sqrt{12})$

$$t_6(y) > -(6y-\tfrac{1}{2}y^3)+3(1-y^2)-\{3+3y^2-y^4\}, \qquad \text{(A 12)}$$

which is positive for $y < \sqrt{12}$. Finally, for $y > \sqrt{12}$

$$t_6(y) > (6y-\tfrac{1}{2}y^3)+3(1-y^2)-\{3+3y^2-y^4\}$$

which is positive for $y > \sqrt{12}$. Hence $t_6(y)$ is positive for $y > 0$.

Thus we have shown T_2/T_1 has a positive imaginary part for $x > 0, y > 0$ and can vanish only when $x = 0$ or $y = 0$. Further when $y = 0, s_0 = x$ and the series form of T_1, T_2 in (2.21) shows that T_2/T_1 is real and positive. Hence T_2/T_1 can achieve real negative values only when $x = 0$, i.e. when s_0 is purely imaginary and s is real and negative as required.

REFERENCES

Batchelor, G. K. 1967 *An Introduction to Fluid Dynamics.* Cambridge University Press.

Clift, R., Grace, J. R. & Weber, M. E. 1978 *Bubbles, Drops, and Particles.* Academic.

Harper, J. F. 1972 *Adv. Appl. Mech.* **12**, 59.

Ockendon, J. R. 1968 *J. Fluid Mech.* **34**, 229.

Sy, F. & Lightfoot, E. N. 1971 *AIChE J.* **17**, 177.

Sy, F., Taunton, J. W. & Lightfoot, E. N. 1970 *AIChE J.* **16**, 386.

Taylor, T. D. & Acrivos, A. 1964 *J. Fluid. Mech.* **18**, 466.

Villat, H. 1943 *Leçons sur les Fluides Visqueux.* Paris: Gauthier-Villars.